Sustainable Cities and Society 130 (2025) 106513

Contents lists available at ScienceDirect

Sustainable Cities and Society

journal homepage: www.elsevier.com/locate/scs

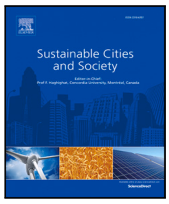

Do urban green spaces cool cities differently across latitudes? Spatial variability and climatic drivers of vegetation-induced cooling☆

Priyanka Rao [a,b,*], Daniele Torreggiani [a], Patrizia Tassinari [a], Thomas Rötzer [b], Stephan Pauleit [b], Mohammad A. Rahman [c]

[a] Department of Agro-Food Sciences and Technologies (DISTAL), University of Bologna, Bologna, Italy
[b] TUM School of Life Sciences, Technical University Munich, Freising, Bavaria, Germany
[c] School of Agriculture, Food and Ecosystem Sciences, The University of Melbourne, Burnley, Victoria, Australia

ARTICLE INFO

Keywords:
Urban vegetation planning
Urban heat island
Cross-climate
Urban cooling
GTB regression
Remote sensing

ABSTRACT

Urbanization transformed global landscapes, intensifying Urban Heat Islands (UHI), further exacerbated by climate change. Sustainable green urban design offers cooling effects through evapotranspiration and shading with varying effectiveness across regions. This study investigates the role of urban vegetation, particularly trees and grassland, in moderating temperatures across nine European cities from 40°N to 53°N, with Temperate to Mediterranean climates. High-resolution Land Surface Temperature (LST) data, downscaled using a Gradient Tree Boosting model, were integrated with the De Martonne Aridity Index and a Contribution Index (CI) to quantify vegetation-driven cooling across a latitudinal gradient. The results show that tree and grassland cooling effects are not spatially uniform: vegetation in cooler, less arid cities provides stronger thermal mitigation. Regression analysis using Random Forest and Generalized Additive Models revealed that vapor pressure deficit (VPD) most strongly influences vegetation cooling, followed by precipitation and solar radiation. Even similar vegetation types demonstrate differing cooling performance depending on local climatic conditions. This study emphasizes the importance of optimizing urban greening strategies to geographic and climate-specific contexts, offering actionable insights for designing climate-responsive green infrastructure to reduce urban heat.

1. Introduction

More than half of the world's population resides in urban areas, projected to reach 70% by 2050 (Leong et al., 2018). Summer temperatures have intensified worldwide, with Europe experiencing a remarkably rapid and faster increase than other regions (Pardo & Paredes-Fortuny, 2024; Tejedor et al., 2024). This is a significant concern as extreme temperatures cause substantial increases in overall mortality rate and adversely affect agriculture, water resources, and ecosystems. The health impacts are especially severe in urban areas. Urban residents are increasingly burdened by extreme heat due to rapid urbanization and global climate change. This exacerbates the formation of urban heat islands (UHIs), areas with significantly higher temperatures in urban areas than their rural surroundings (Krayenhoff, Moustaoui, Broadbent, Gupta, & Georgescu, 2018; Mora et al., 2017). UHI-based studies have shown that the intensity of UHIs, varying between 0.8 to 9.0 °C during single days (Hartmann et al., 2023; Manoli et al., 2019), and is more pronounced during summer, typically at night (Gartland, 2012; Rao, Tassinari, & Torreggiani, 2024b). This variation is influenced by factors such as urban size, local climate, urbanization gradients, and impervious surface areas (Estoque, Murayama, & Myint, 2017; Varquez

☆ The research has been carried out within the PhD project "Big data and healthy cities: regeneration of urban contexts, green systems and safe and healthy lifestyles", funded by the Emilia-Romagna Region (Italy) within the Research training projects "Big Data per una regione europea più ecologica, digitale e resiliente" (Fondo POR FSE—Resolution n. 752 of 24 May 2021).

Funded by the European Union - NextGenerationEU under the National Recovery and Resilience Plan (PNRR) - Mission 4 Education and research - Component 2 From research to business - Investment 1.1 Notice PRIN 2022 PNRR (DD N. 1409 del 14/09/2022), from title [Urban green systems: integrated modelling of environmental, energy and microclimatic benefits and GHG offsetting for strengthening resilience and adaptation to climate change – GRACE (Green foR climAte resilience)], proposal code [P20229ZC79] - CUP [J53D23018250001]."

Thanks also go to the German Research Foundation (Deutsche Forschungsgemeinschaft) for providing funds for the project 437788427 - RTG 2679.

* Correspondence to: Department of Agro-Food Sciences and Technologies (DISTAL) Alma Mater Studiorum - Universitá di Bologna, Viale Giuseppe Fanin, 48, 40127 Bologna BO, Italy.
E-mail addresses: priyanka.rao2@unibo.it, priyankarao2413@gmail.com (P. Rao).

https://doi.org/10.1016/j.scs.2025.106513
Received 9 January 2025; Received in revised form 29 April 2025; Accepted 1 June 2025
Available online 18 June 2025

& Kanda, 2018). However, there is a gap in understanding how these varied UHI findings can be effectively applied to urban interventions, such as green infrastructure, to reduce urban heat across global cities with varying climate and weather conditions (Manoli et al., 2019).

Urban green spaces (UGS) can lower temperatures in their vicinity through evapotranspiration, shading, and increased albedo, which measures how much solar energy a surface reflects (Bowler, Buyung-Ali, Knight, & Pullin, 2010). Various types of UGS, including parks, grass, green roofs, and green walls, have been extensively researched and highlighted as strategies for mitigating UHI effects. These studies have employed different methods like field measurements, remote sensing, and model simulations (Balany, Ng, Muttil, Muthukumaran, & Wong, 2020; Bartesaghi-Koc, Osmond, & Peters, 2020; Saaroni, Amorim, Hiemstra, & Pearlmutter, 2018). The urban morphological setting and UGS have been extensively studied recently. For instance, it has been found that the size of the green area is critical in reducing heat (Zhang, Ge, Wang, & Dong, 2025). The cooling effect of green–blue spaces varies with landscape density. In low-density areas, dispersed green–blue spaces are more effective, while large and organized green–blue spaces are necessary in high-density areas (Sheng & Wang, 2024). The inequality in cooling adaptation depends on disparities in green space quality and quantity, driven by factors such as socioeconomic conditions, urban morphology, and environmental characteristics (Li et al., 2024). Further in another study (Xu, Jin, Ling, Sun, & Wang, 2025), green space morphological spatial patterns have been found to negatively impact the UHI intensity with "core" areas being the most effective in reducing UHI. Assessing the combined effect of urban buildings and green spaces on the urban thermal environment (Chen et al., 2023; Kim, Yeom, & Hong, 2025) showed that integration of high-rise building and green spaces together mitigates the UHI significantly. Whereas compact low-rise and heavy industry areas contribute the least to the cooling benefits (Liu et al., 2024). However, the cooling effect of UGS varies significantly depending on the functional type of green space along with surface roughness and climatic and edaphic variables such as atmospheric dryness, and soil moisture (Manoli et al., 2019). In general, trees with higher and denser canopies provide shading, which reduces ground heat flux and lowers surface temperature. Additionally, they influence convection, therefore reducing the air temperature (Rahman et al., 2021). Simultaneously, trees with many layers of leaves transpire significantly more compared to grass or shrubs, hence, higher air cooling (Rahman, Moser, Rötzer, & Pauleit, 2019). Thus, urban trees generally contribute more significant cooling than grasslands (Bartesaghi-Koc et al., 2020), especially at higher temperatures and in drier climates (Manoli et al., 2019). However, the intensity of cooling can vary considerably even within the same cities (Pattnaik et al., 2024). Despite this, most studies on UGS cooling effects are still limited to specific locations and particular types of green spaces. Additionally, the use of non-comparable methods (Balany et al., 2020; Bartesaghi-Koc et al., 2020; Koc, Osmond, & Peters, 2018), restricts the ability to generalize findings across diverse urban areas globally. For example, seasonal cooling from green–blue infrastructure varies with its width and area, while is strongest near blue spaces. The cooling follows a gradient in buffer zones and differs in agricultural areas based on urban proximity (Abd-Elmabod, Gui, Liu, Liu, Al-Qthanin, Jiménez-González, & Jones, 2024; Zhao et al., 2023).

Studies on urban thermal environments have followed various approaches over time. Traditional approaches relied on ground-based measurement devices, like spectroradiometers, which required physical presence at each study location (Thome, 2001). However, remote sensing techniques, which allow for global data capture without direct contact, have largely replaced these methods. Satellite images obtained through remote sensing provide macroscale data, covering large areas, and facilitating global-scale studies (Guo, Zhang, & Zhu, 2015). While collecting global data using ground measurements for the same time period is challenging, satellite datasets make this process easier, faster, and more cost-effective. Land Surface Temperature (LST) is a crucial parameter for studying the impacts of climate change and identifying temperature anomalies across various scales (Li & Duan, 2018). It is widely used in Surface Urban Heat Island (SUHI) studies, offering more detailed insights than meteorological stations, which primarily measure near-surface air temperatures. Unlike atmospheric UHI (estimated using air temperature), SUHI is less complex as it primarily depends on surface properties and materials (Pyrgou, Hadjinicolaou, & Santamouris, 2020). The advancement of thermal remote sensing has enabled satellite data to provide information on UHI with spatial resolutions ranging between 30 m and 500 m (Weng, 2009). Satellites such as Landsat, Sentinel, MODIS, and ASTER are commonly used for LST studies (Rao, Singh, & Pandey, 2021; Rao, Tassinari, & Torreggiani, 2024c; Wulder et al., 2016). The first satellite-based UHI observations were made by Krishna (1972), and since then, many researchers have developed various methods to assess LST and UHI variability (Imhoff, Zhang, Wolfe, & Bounoua, 2010; Tran, Uchihama, Ochi, & Yasuoka, 2006; Yue, Liu, Zhou, & Liu, 2019).

However, the application of remote sensing methods used for studying UHIs at a landscape scale is often limited due to the small-scale implementation of UGS in actual urban settings. While field measurements and empirical observations of air temperature using sensors, weather stations, and thermistors provide direct insights into UGS's immediate and actual effects on temperature (Bowler et al., 2010), this approach is expensive and time-consuming when applied globally (Kim, Khouakhi, Corstanje, & Johnston, 2024). Satellite-derived LST is available at a 30-meter resolution, which is often too coarse to detect thermal stress within spatially heterogeneous urban landscapes. Recent studies have employed machine learning models to downscale satellite-derived LST to analyze urban thermal stress. In this study, we adopt a similar approach, producing high-resolution LST at a 10-meter resolution using Landsat-derived LST and Sentinel-derived land use land cover indices. These innovations, alongside further integration of machine learning and deep learning techniques, e.g., dataset fusion for higher spatial/temporal resolution (Rao, Tassinari, & Torreggiani, 2024a; Yao, Chang, Ndayisaba, & Wang, 2020), lead to an enhanced understanding of UHI mechanisms and their interaction with urban landscapes.

To effectively use urban green spaces, particularly tree planting, to address environmental injustices and health risks from rising temperatures across different climate settings. It is equally important to quantify how urban trees, in turn, influence local climate conditions. Recent studies have highlighted different functionality of the green spaces under varying climate conditions (Rahman et al., 2024). This variation makes it impractical to apply a uniform standard for green coverage and urban green space types across all climates. For example, the study done by Schwaab et al. (2021) concluded that variations in the cooling effects of vegetation were observed in cities with diverse climate types. The study found that urban trees significantly reduced LSTs, with the most significant reductions observed in Central Europe and smaller effects noted in Southern Europe. In drier climates, where water availability is limited, the cooling mechanisms of UGS shift, with shading becoming more crucial than transpiration. This is because trees, when exposed to high evaporative demand and limited soil moisture, often reduce transpiration to avoid hydraulic stress. As a result, the cooling effect of evapotranspiration diminishes during the hottest period of the day (Paudel, Naor, Gal, & Cohen, 2015; Rahman et al., 2021). Instead, shading from tree canopies plays a dominant role in cooling by significantly reducing solar radiation and providing thermal comfort, especially in regions where water availability is constrained (Bush et al., 2008; Martin-StPaul, Delzon, & Cochard, 2017; Shashua-Bar et al., 2023). This highlights the importance of shade in dry climates, where trees close their stomata to conserve water, limiting transpiration and causing cooling from shading to become the primary mechanism (Cheng, Peng, Dong, Liu, & Wang, 2022; Oren et al., 1999). As the cooling effects of urban trees differ based on climate type, trees in Mediterranean climates have different cooling effects (Seager et al.,

2019) compared to those in temperate or tropical climates (Cheung, Livesley, & Nice, 2021). In both climate regions, more precipitation amplifies the cooling impact of grass-covered green spaces (Cheung et al., 2021). Consistently, urban trees in arid areas may require more water and management than those in more humid environments (Cheng et al., 2022). Studies have shown that transpirational cooling is more influential in temperate climates (Rahman et al., 2024, 2020); however in hot, dry regions, shading should be the primary consideration when planting trees, as it provides the most effective cooling where trees are more adapted to dry climate and stomatal resistance is high for transpiration cooling (Shashua-Bar et al., 2023).

Given the variation in climate with latitude gradient, this research aims to investigate whether there is a relationship between the impact of similar vegetation types within a latitudinal gradient of about 15°. As highlighted, the cooling benefits of trees, even within the same functional type, can vary significantly due to the influence of the soil–water–atmospheric continuum. Furthermore, urban topography, street orientation, and surrounding environmental geometry might influence this continuum, resulting in below-par cooling potential from UGI (Rahman et al., 2024). Therefore, major cities across a latitudinal gradient with similar vegetation functional types will help to understand the impact of climatic variables, for instance, the temperature and moisture, when planning multifunctional UGI for current and future cities.

Hence, this study adopts a spatially structured fine-scale approach that is situated between global macroscale assessments and localized park-scale analyses. It investigates intra-urban variations across a latitudinal gradient, introduces a modified contribution index, and integrates climatic variables (VPD, precipitation, and solar radiation) using GAM and RF models to assess how climate mediates urban vegetation cooling, which is often missing in broader-scale studies.

Henceforth, the following are the main objectives of this study to address the research gaps highlighted:

1. To spatially evaluate vegetation-induced cooling effects within urban boundaries, comparing the efficacy of different vegetation types in mitigating urban heat across different populated cities.
2. To investigate the climatic influence on the urban vegetation-led cooling mechanism in different European cities across a 10–15° latitudinal gradient.

The following sections of the paper are as follows: Section 2 consist of details about the study area and methodology applied. Further, Section 3 consists of the results, followed by sections 4 of discussions and 5 of conclusions.

2. Methods

2.1. Study area

The case study focused on nine European cities across a latitudinal gradient from 40°N to 53°N in the Northern Hemisphere Fig. 1. The selected cities provide a diverse geographical context to analyze how different plant communities that can thrive under varying environmental conditions but exhibit similarities in their overall structure contribute to cooling in various climate conditions and their role in mitigating UHI effects. The generalized vegetation types include deciduous trees (European oak, silver birch, and common hornbeam) which are well adapted to temperate climates; coniferous trees (Scots pine and Norway spruce) often used for aesthetic value and generally found in parks and urban green spaces; ornamental trees and shrubs (flowering cherry, common lilac and Norway maple) to enhance biodiversity; native and adapted species (European hornbeam, English Elm, and lime) found in urban settings to provide resilience to pollution and adaptivity to varying soil conditions; Mediterranean species (Aleppo pine, holm oak, and Mediterranean cypress), particularly found in southern cities amongst the case study selected cities, and are more drought resistant and well-suited for warmer and drier climates. The cities—Hamburg, Hannover, Würzburg, and Munich in Germany; Budapest and Szeged in Hungary; and Milan, Imola, and Naples in Italy. Fig. 1 —span a range of climates from temperate oceanic to humid subtropical to hot Mediterranean, according to the Köppen-Geiger classification.

The German cities Hamburg (53°N), Hannover (52°N), Würzburg (49°N), and Munich (48°N) are characterized by temperate oceanic climates (Cfb), with relatively mild summers and winters. The urbanization level in Hamburg is high, with a dense urban fabric, numerous parks, and green spaces interwoven within its landscape (can be witnessed in the LULC distribution across the spatial gradient: Fig. 4). Further, Hannover's urbanization is characterized by a mix of residential, industrial, and commercial areas with significant green infrastructure. The city's climate resembles Hamburg's, with mild to warm summers and relatively moderate winters. Moving further south, Würzburg is located at 49°N in Bavaria and has a temperate oceanic climate (Cfb), though it is closer to the border of a humid subtropical climate (Cfa). Würzburg's landscape is dominated by vineyards and rolling hills, reflecting a region where agricultural land use is significant. The urbanization in Würzburg is moderate (based on Fig. 4), with a blend of historical architecture and modern developments. The city's climate is slightly warmer and drier than the northern cities. Munich, located at 48°N, also in Bavaria, experiences a temperate oceanic climate (Cfb) with continental influences. The city is known for its high level of urbanization and extensive green spaces, including the famous Englischer Garten, one of the largest urban parks in the world. These cities, particularly Hamburg and Munich, have extensive urban green spaces crucial for mitigating UHI effects. The maritime influence in northern cities like Hamburg contrasts with the more continental climate of Munich, offering an opportunity to explore how these differences affect the cooling potential of urban vegetation.

In Hungary, Budapest (47°N) and Szeged (46°N) experience humid subtropical climates (Cfa) with significant continental influences, leading to hot summers and cold winters. Budapest, being a densely urbanized capital city, and Szeged, with its sunnier and warmer climate, provide distinct settings to examine how vegetation can alleviate the intense UHI effects typical of such climates. The Italian cities Milan (45°N) and Imola (44°N) also have humid subtropical climates (Cfa) but differ in their levels of urbanization. Milan, a major industrial hub with significant urban sprawl, contrasts with the smaller, less urbanized Imola, which features a mix of land uses, including industrial and agricultural areas. These cities offer insights into how vegetation can be leveraged to cool urban environments in highly industrialized areas versus less dense settings. In addition, Naples has a Mediterranean climate, featuring hot, dry summers and mild, rainy winters. The area's climate is well-suited for cultivating crops such as olives and grapes, with the Tyrrhenian Sea playing a key role in shaping the local weather patterns. The city is dense, blending historical districts, industrial zones, and modern developments. Suburban sprawl has also extended beyond the core city, contributing to pressure on transportation and housing.

Collectively, these cities provide a comprehensive framework for studying the interplay between vegetation, climate, and urbanization across different latitudes, helping to identify strategies for optimizing the cooling effects of greenery in urban areas.

2.2. Datasets used

This study expands across multiple cities along the latitudinal gradient; therefore, satellite-derived land surface temperature has been used to acquire thermal data. Landsat is the freely available data with the thermal band to calculate the LST with the highest spatial resolution, i.e., at 30 m resolution. Still, this resolution is coarse in capturing the details of the landscape for small-scale urban settings. Therefore, the case study used a novel regression model approach to downscale the Landsat-derived LST from 30 m to 10 m resolution.

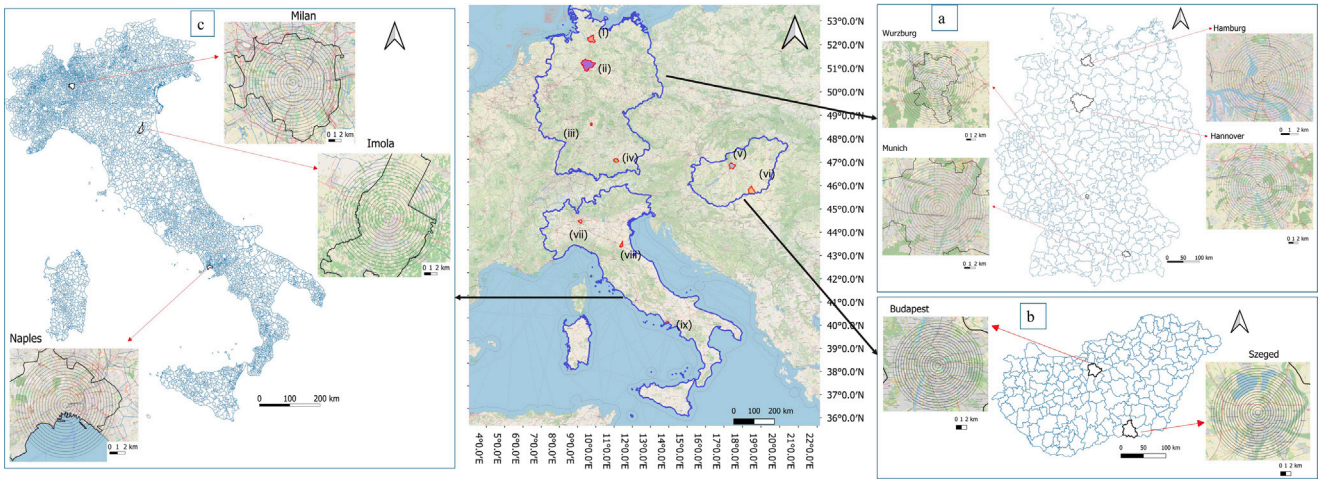

Fig. 1. Cities analyzed along the latitudinal gradient, where (i) Hamburg (53°N), (ii) Hannover (52°N), (iii) Wurzburg (49°N), (iv) Munich (48°N), (v) Budapest (47°N), (vi) Szeged (46°N), (vii) Milan (45°N), (viii) Imola (44°N), and (ix) Naples (40°N). Where (a) denotes cities in Germany, (b) cities in Hungary, and (c) cities in Italy. All the cities have been zoomed at the concentric buffers (up to 8.5 km from the center).

Table 1
Data specifications.

Data type	Source/Detail	Resolution/Details	Time period	Purpose
City Boundary	ADM level 3 shapefile	Highest scale available	Most recent available	Defining LST downscaling boundary
Satellite Data	Google Earth Engine (GEE): Landsat 8/9, Sentinel-2	30 m (Landsat), 10 m (Sentinel)	One day of August month in 2022–2023 (varies by cloud cover)	LST calculation, model training, land use indices
Land Cover Data	GEE: Sentinel LULC	10 m	2021	Assess LULC type and area coverage
Weather Data	Various portals: DWD (Service, 2024a); Hungry weather data portal (Service, 2024b); Lombardy weather data portal (Geoportal, 2024); Emilia-Romagna weather data portal (Emilia-Romagna, 2024); Campania weather data portal (Portal, 2024).	Annual averages, hourly measurements	Same day as the LST data	Used for calculating independent variables in the regression model
Tools	GEE, GIS software (QGIS 3.28.8; ArcGIS Pro), Python geospatial packages	–	–	Data processing, analysis, and modeling.

Further weather data like annual precipitation, hourly solar radiation, air temperature, and relative humidity have been acquired from the weather portals of the respective country and region to assess the relative importance of several climatic and weather parameters towards the urban vegetation-led cooling effect. The data specifications are listed in Table 1.

Fig. 2 demonstrates the step-by-step workflow of the study. This study investigates the impact of urban vegetation on surface temperature regulation across a city, from the center towards the periphery, up to an 8.5 km radius, to analyze the LULC spatial distribution in the cities across the latitudinal gradient depicting varied climatic characteristics. The distance from the center to the periphery was uniformly fixed for all the cities, as the urban periphery of many investigated cities is not well demarcated beyond 8.5 km.

This approach was adopted to ensure comparability within the cities and to compare the urban to peri-urban transitions uniformly. Cities were selected along a continuous latitudinal gradient (40°N–53°N) within a narrow longitudinal band in Europe, ensuring climatic consistency and comparable land use patterns to isolate vegetation-driven cooling effects. City size was not a selection criterion, as the focus was on capturing latitudinal and climatic variation in a spatially controlled manner. The methodology integrates the downscaling of LST, spatial analysis of land use types, landscape and climate-based indices, and assessing climatic parameters to evaluate urban cooling effects along a latitudinal gradient. The methodology can be broadly divided into four phases, each assessing either climate variable or landscape-type spatial analysis to thermal variability.

2.3. Super-resolving Land Surface Temperature (LST)

The first phase of the study focused on the downscaling of LST data. The downscaling process consists of utilizing the regression model that was trained on Landsat −8 derived indices (NDVI, NDBI, NDWI) and LST data at 30 m spatial resolution to predict the higher-resolution LST at 10 m spatial resolution using the Sentinel-2 derived indices (NDVI, NDBI, NDWI). The insights of using these three indices for super-resolving LST is based on the previous study (Rao et al., 2024a).

Cloud-free satellite data from August 2022 and 2023 was identified to ensure data quality. Using Landsat 8/9 imagery, the LST was calculated. A Gradient Tree Boosting (GTB) regression model was then trained using this Landsat-derived LST and land use indices. This approach is replicated based on a previous study, upgrading the regression model (Rao et al., 2024a). This model was subsequently employed to predict LST for another nearby date with available cloud-free Landsat

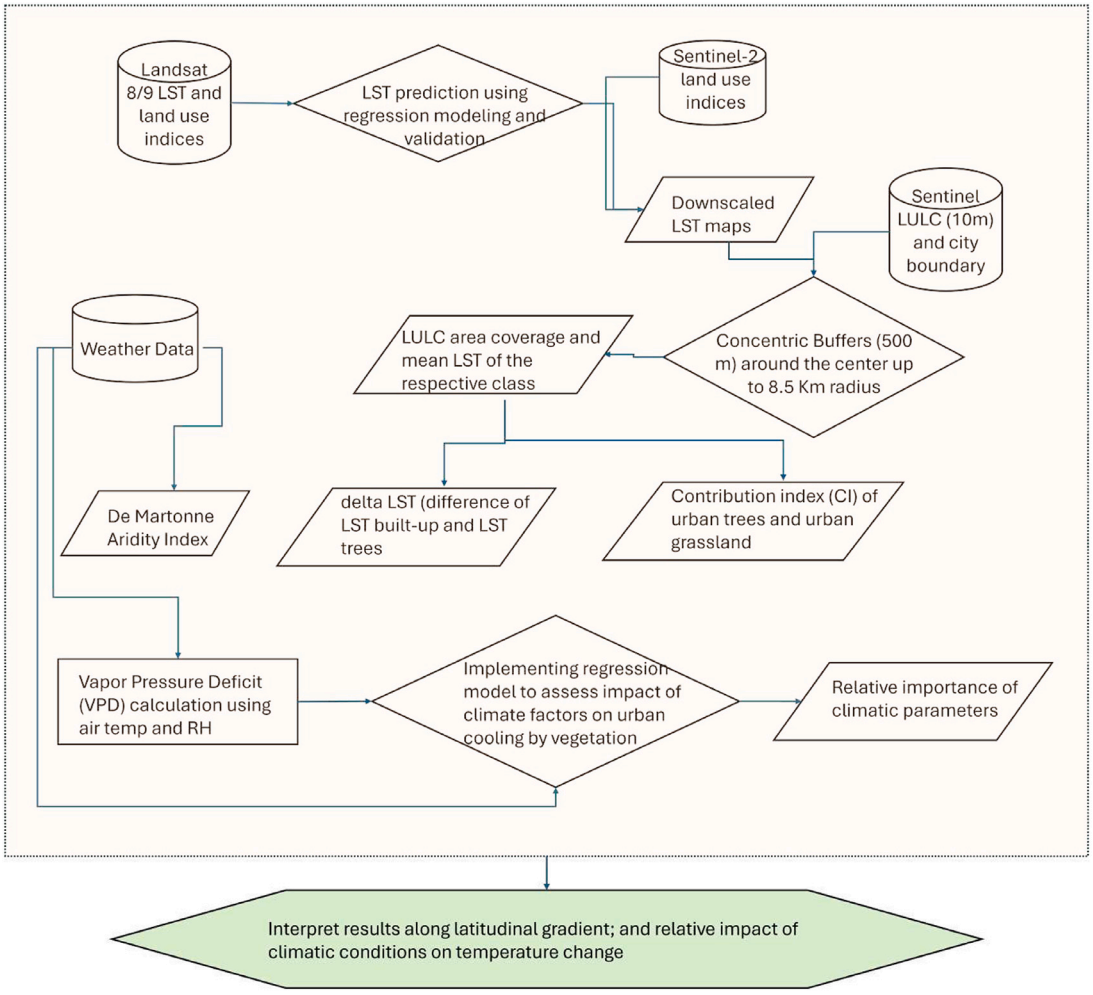

Fig. 2. Step-by-step method flow chart, where the computational link and source data have been explained for each variable used in the study.

data. The trained model was then validated against directly calculated Landsat LST values, achieving satisfactory accuracy. Following validation, the model was employed to predict the LST at a finer spatial resolution of 10 m using Sentinel-2-derived land use indices. The final downscaled LST maps were downloaded, marking it as the output of the first phase.

Algorithm 1 (refer to supplementary material, algorithm1), explains the training of the GTB model for downscaling the LST. GTB was preferred for this task because of its characteristics in modeling non-linear relationships and its capture of complex patterns and interactions between variables, leading to more accurate and robust predictions.

2.4. Quantification of UGS contribution at the urban and latitudinal gradient

Further, spatial analysis was performed using each city's downscaled LST maps and Sentinel-derived LULC data. Concentric buffers with a radius of 500 m were generated around the city center, extending up to 8.5 km within the city boundary. The 500 m scale is consistent with the previous urban climatology studies (Cao, Onishi, Chen, & Imura, 2010; Zhu et al., 2021). Each buffer's area coverage of different LULC types (tree cover, grassland, built up, and others) and the corresponding mean LST for each class were calculated. The modified Contribution Index (CI) quantifies the relative effectiveness of each land cover type (trees, grassland, etc.) in cooling urban areas, normalized per unit of area. Many studies have focused on absolute LST differences; however, CI allows us to evaluate how effectively a land cover type contributes to cooling within a defined urban space. The modified CI was defined as:

$$CI = \frac{(LST_{\text{class}} - LST_{\text{mean}})}{Area_{\text{class}}} \quad (1)$$

In Eq. (1), LST_{class} is the LST of a specific LULC type, LST_{mean} is the mean LST across all LULC types within a buffer (ring area), and $Area_{class}$ is the area coverage of that specific LULC type. The CI formulation is adapted and modified from the framework proposed by Ayanlade, Aigbiremolen, and Oladosu (2021), who originally used LST differences weighted by land cover proportions. In our modified formulation, CI is calculated as the difference between the LST of a specific land use/land cover (LULC) class and the mean LST of the buffer zone, normalized by the area of that LULC class within the buffer. Dividing by the area of the land cover type helped us to understand whether small green spaces provide disproportionately strong cooling effects (i.e., cooling efficiency), that is, per-unit area based analysis. This approach aligns with urban planning goals, where maximizing cooling benefit per unit area is essential due to limited land availability. In addition, it also helped normalize across buffer zones. These CI values were plotted across the buffers to assess these vegetation types concerning their role as sinks or sources of the urban temperature, spatially varying from the city center to its periphery. These CI values were plotted for all the cities at different latitudes to analyze this relation along the latitudinal gradient.

The delta of temperature difference between each type of urban vegetation (tree cover and grassland) and built-up, referred to as Delta LST from here, was calculated at the whole-city level for each city,

Fig. 3. Downscaled LST visualization in comparison to coarser resolution (Landsat derived) LST, along with the reference of Open Street Map (OSM) for the Englischer Garten and nearby area of Munich. Only one small area of a city has been shown for representation purposes.

to assess the thermal stress in the built-up areas. In addition, the De Martonne Aridity Index (DAI) was calculated to assess climatic aridity across each city, based on the formula given by Mavrakis and Papavasileiou (2013). The DAI is defined as:

$$DAI = \frac{P}{T + 10} \tag{2}$$

In Eq. (2), P is the annual precipitation (mm), and T is the temperature (in °C). The DeltaLST and DAI were plotted across latitudinal gradients to identify trends and correlations between temperature differences and climatic aridity. Further, vapor pressure deficit (VPD) was calculated for each city using the following formula, as it measures how much more moisture the air can hold relative to what it currently has.

$$SaturationVaporPressure(ES) = 0.61078 * exp\frac{(17.27 * T)}{(T - 237.15)} \tag{3}$$

$$ActualVaporPressure(EA) = \frac{(RH)}{(100)} * ES \tag{4}$$

$$VaporPressureDeficit(VPD) = ES - \frac{(RH * ES)}{(100)} \tag{5}$$

In Eqs. (3), (4), (5), T is the air temperature in °C; RH is the relative humidity in %.

2.5. Statistical modeling and analysis

A combination of Generalized Additive Models (GAM) and Random Forest (RF) regressors have been utilized to analyze the impact of several environmental variables—namely, Precipitation, Solar Radiation, VPD, and Latitude—on the variation of delta LST across different cities. For this analysis, we have focused on delta LST calculated as temperature difference between built-up and trees. Their complementary strengths drove the choice of these two models: while GAM allows for the modeling of non-linear relationships and provides interpretability through smooth functions, RF offers a robust approach that can handle complex interactions between variables without prior assumptions about their form. In addition, several other models were applied to the data, such as the support vector machine and gradient boost regression model, but these models could not perform well due to less data.

For the RF model, we used 100 trees with a random state set to 42 for reproducibility. Random Forest is well-suited for capturing complex interactions between features due to its ability to fit multiple decision trees on various subsamples of the dataset. The GAM, on the other hand, allowed us to model the response variable as a smooth, non-linear function of the predictors. We included smooth terms for each of the four variables in the GAM, and the model fitting was performed using the 'pygam' library in Python. The result was evaluated using standard performance metrics, including R-squared, Mean Absolute Error (MAE), and Root Mean Squared Error (RMSE). Additionally, for the GAM, we assessed the statistical significance of the predictors using p-values. All these explained statistical analyses were carried out on Google Colab for fast and seamless computations. All plots and results were analyzed along the latitudinal gradient to interpret the spatial variability and the relative impact of climatic conditions on urban cooling, emphasizing the role of vegetation.

3. Results

3.1. Super resolved land surface temperature

The model developed using the GTB regression approach effectively downscaled LST to a 10-meter resolution using NDVI, NDBI, and NDWI as predictors. Fig. 3 demonstrates the difference between Landsat-derived LST and super-resolved LST for a part of Munich city in the spatial domain and compares the detailing level between the two datasets. The validation process, involving the prediction of LST for different dates, demonstrated the model's robustness. The predicted LST values were compared to LST derived directly from the Landsat thermal band, yielding consistent and strong performance metrics. The model's correlation coefficient consistently exceeded 0.7 across all validation checks, with specific metrics showing a correlation coefficient of 0.8469, an R-squared value ranging from 0.61 to 0.72, a p-value of <0.001, and a standard error of 0.0005. This strong correlation indicates the model's reliability in capturing the relationship between LST and the predictor indices and the underlying trends and patterns between the variables.

3.2. Urban land cover distribution and surface temperature

The proportion of LULC types present in an area is one of the parameters for explaining the existing thermal conditions in an urban or rural setting. Therefore, Fig. 4 consists of bar graphs for studied cities, illustrating the percentage area of LULC types within buffers of increasing distance from the city center at the interval scale of 500 m and the mean LST for the selected summer day in August 2022 and 2023. The LULC types are categorized as tree cover (green), grassland (yellow), built-up area (red), and other types (gray). The bar graphs reveal a clear trend across all cities: built-up areas dominate near the city centers, contributing to higher mean LST, while tree cover increases with distance from the center, leading to a decrease in mean LST. This pattern highlights the significant role of tree cover in mitigating urban heat.

In most cities, such as Hamburg, Hannover, Munich, and Milan, the percentage of built-up areas is high near the center, often around 70%–80%, and decreases steadily with distance. In contrast, tree cover is low but increases significantly beyond 4.5 km from the center. The increase in tree cover coincides with a noticeable reduction in mean LST, emphasizing the cooling effects of vegetation. In Hamburg, the reduction in temperature has been more pronounced in areas with higher tree cover, demonstrating a significant cooling trend with increased tree density. Similar trends are observed in Hannover, Munich, and Milan, where reductions in mean LST align with areas of greater tree cover, suggesting a direct relationship between LULC and local thermal conditions. This pattern is also evident in Wurzburg, where the higher percentage of tree cover near the city center leads to a more consistent reduction in LST, compared to other cities with varying tree distributions. In Budapest and Szeged, localized decreases in mean LST coincide with areas of increased vegetation, while in Napoli, lower vegetation

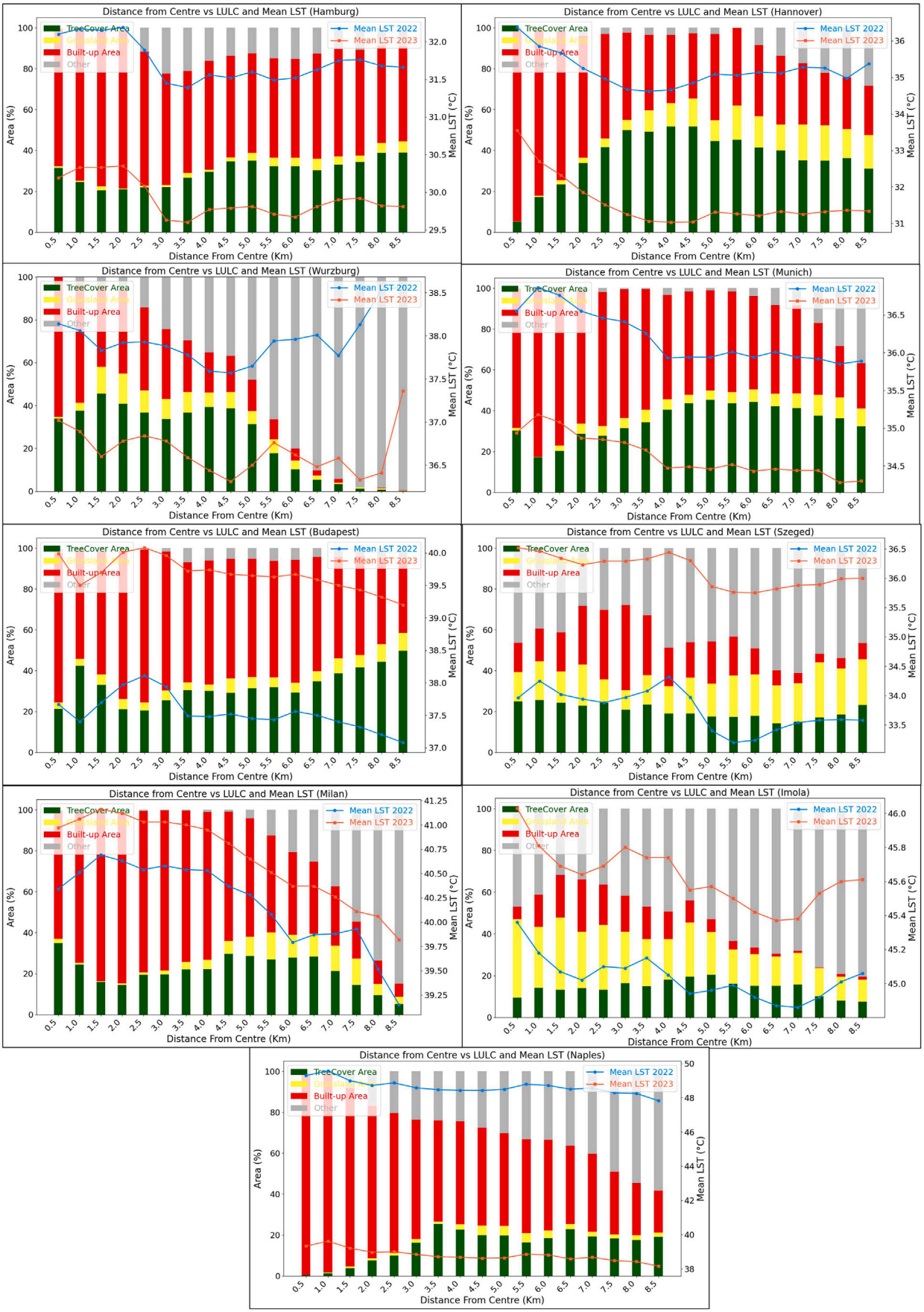

Fig. 4. Mean LST and LULC composition from city center buffer to periphery in cities between 53°N and 40°N latitude. The mean LST shown here represents a single-day observation in August of 2022 and 2023 (based on the availability of cloud-free satellite data for LST estimation). The color legend follows: green represents tree cover, yellow represents grassland, red represents built-up, and gray represents other categories.

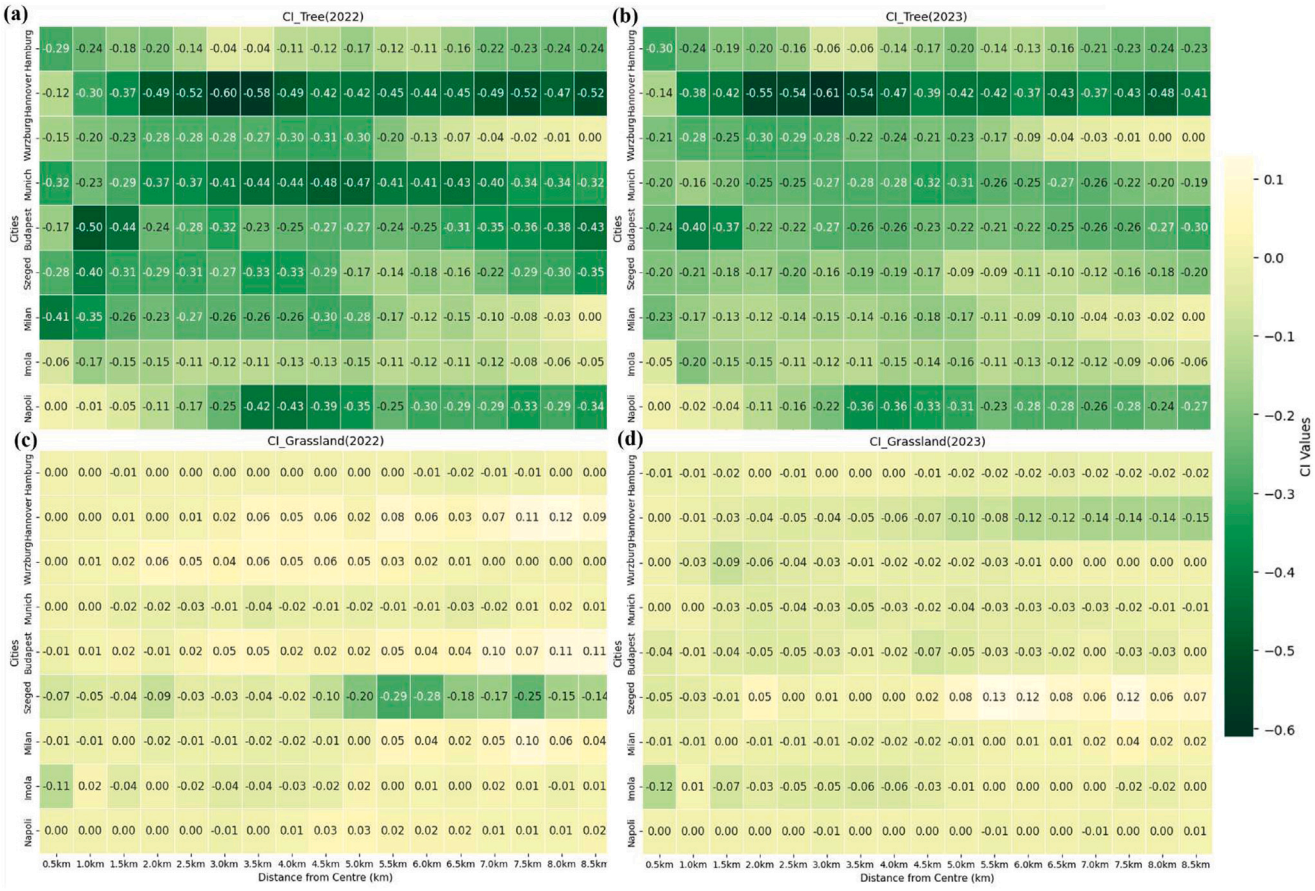

Fig. 5. Contribution Index (CI) across latitudinal gradient ranging between 53°N to 40°N where (a), (b), (c) and (d) represents CI of Tree on the specific day of August in the year 2022, CI of Trees on particular day of August in the year 2023, CI of Grassland on specific day of August in the year 2022, and CI of Grassland on specific day of August in the year 2023, respectively. The top row to bottom row in each heat map represents the nine cities (namely: Hamburg, Hannover, Wurzburg, Munich, Budapest, Szeged, Milan, Imola, and Napoli) located between 53°N and 40°N latitude.

cover in the center coincides with the elevated thermal conditions. Across all cities, these patterns highlight the relationship between tree cover and temperature, showcasing the impact of vegetation type and its coverage in mitigating heat stress.

3.3. UGS Contribution Index analysis within urban boundaries

Fig. 5 consists of four heat maps (as subplots) depicting the CI for trees and grasslands along a latitudinal gradient from 53°N to 40°N. The *y*-axis lists nine cities (Hamburg, Hannover, Wurzburg, Munich, Budapest, Szeged, Milan, Imola, and Napoli) arranged from top to bottom, and the *x*-axis represents the distance from the city center, ranging from 0.5 km to 8.5 km with increments of 0.5 km. This index helps to examine whether a landscape, in relative terms, acts as a thermal sink (landscape type contributing most towards reducing LST) or a thermal source (landscape type contributing relatively very low towards LST reduction). Lower CI values indicate that the landscape is a sink to urban LST, contributing to cooling effects. In contrast, positive CI values suggest that the landscape acts as a source, contributing to urban heat.

Subplots Figs. 5a and 5b, which illustrate CI values for trees in August 2022 and 2023, show a more negative trend as the distance from the city center increases. This indicates a significant cooling effect of trees and their role as thermal sinks. In 2022, Szeged exhibited the most pronounced low CI at 4.5 km from the city center (−0.5), followed closely by Budapest with a CI of −0.58 at 3.5 km. However, by 2023, both cities experienced a reduction in their cooling effect. In contrast, Hamburg consistently demonstrated a stable cooling effect across the spatial gradient in both years, with a slight increase in 2023, reflected by CI values of −0.61 at 3.5 km and −0.54 at 4.5 km from the city center.

Subplots Figs. 5c and 5d display the CI values for grasslands in August 2022 and 2023. The grasslands exhibit minimal influence on LST, with CI values generally near zero, indicating their limited role in cooling. Although the plots show a light green to yellow color gradient, localized cooling effects are observed in Würzburg, Hannover, and Szeged, where slightly lower CI values (−0.28, −0.14, and −0.15, respectively) are recorded. However, these low CI values are minor compared to those associated with tree cover. The overall trend remains consistent across both years, underscoring that grasslands contribute less significantly to heat stress mitigation than trees during daytime.

3.4. UGS surface temperature intensity and aridity index

Generally, grassland has a comparatively less significant impact on cooling; therefore, analyzing the thermal difference between trees and grassland compared with the built-up would estimate the quantified cooling potential of trees and grassland. Considering the assessment to understand the UHI dynamics, Fig. 6 compares the LST differences between built-up areas and two types of land cover, calculated for the entire city: tree and grassland. Delta-LST, the difference in temperature between built-up areas and tree cover versus built-up areas and grassland, measures the cooling potential of these vegetation types in urban environments. It highlights the relationship between Delta-LST and the

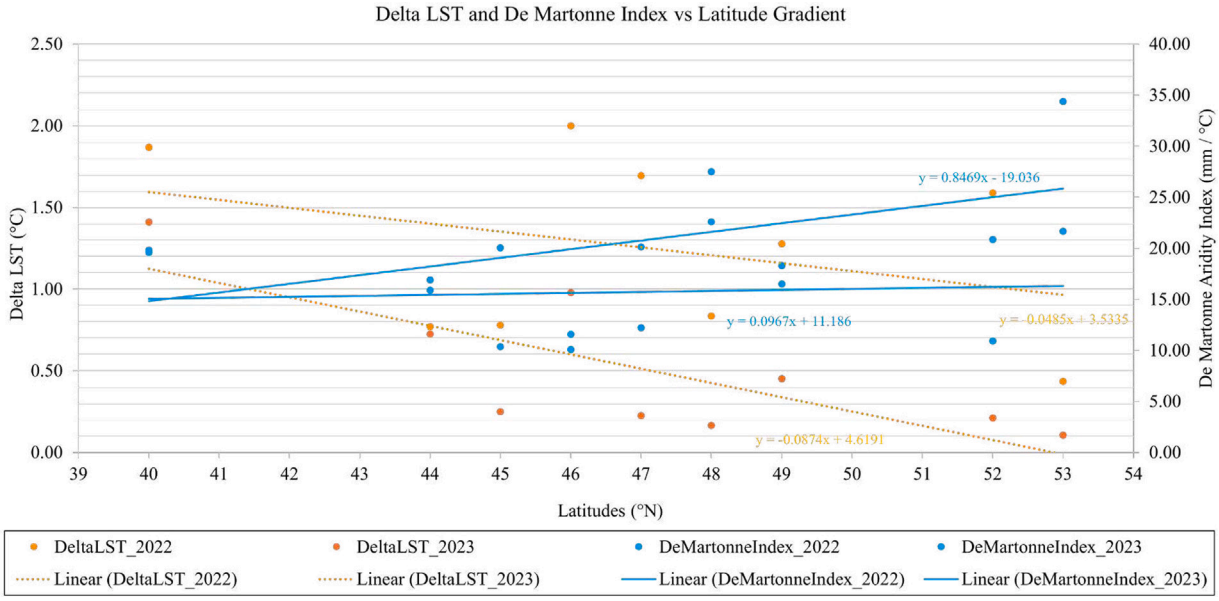

Fig. 6. Delta-LST denoting LST difference between built-up-tree and built-up-grassland; and De Martonne Aridity Index (DAI) concerning the Latitudinal gradient ranging between 53°N to 40°N across different cities representing varying climate characteristics.

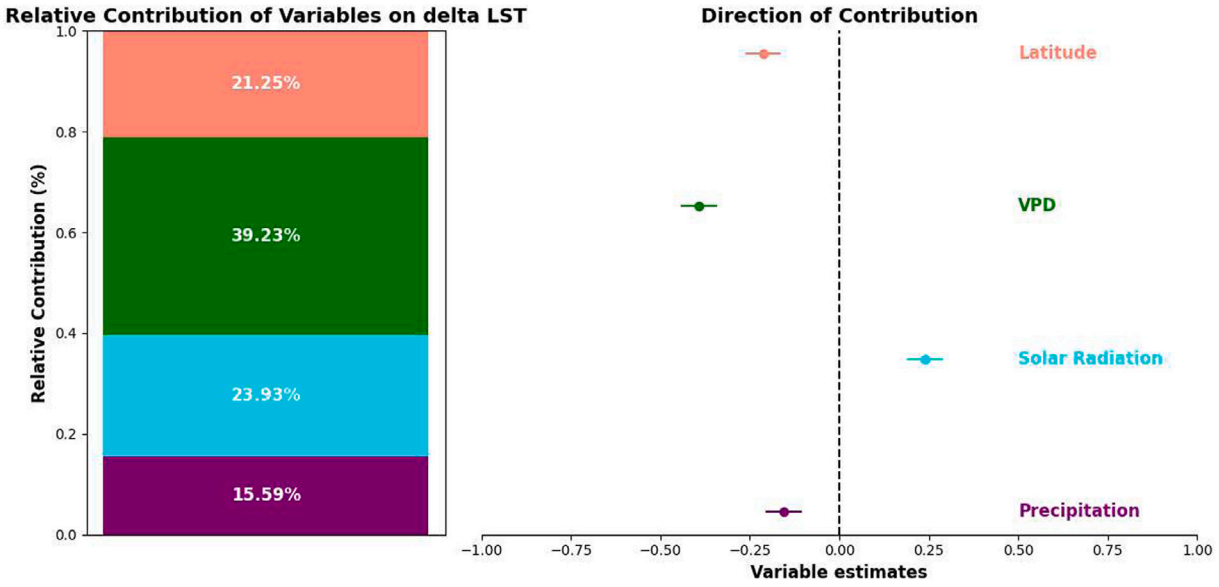

Fig. 7. Relative importance and variable impact of delta LST (temperature difference between built-up and trees) based on integrative modeling approach.

DAI across a latitudinal gradient between 53°N and 40°N. Usually, the climate shows a less arid and more humid trend while moving away from the equator, also indicated by the De Martonne Aridity Index plot. This shift in aridity and climate also correlates with the effectiveness of the urban trees and the grassland from higher to lower latitudes, demonstrated by Delta-LST.

3.5. Modeling for relative contribution of different variables over vegetational cooling

The relative importance plot (Fig. 7) aids in analyzing and visualizing the contribution and impact of various climatic factors (precipitation, solar radiation, VPD) and latitude on the change in the delta LST (representing the urban vegetation cooling, calculated as the temperature difference between built-up and trees). The multicollinearity among the independent variables was assessed using a Variance Inflation Factor (VIF) analysis. The VIF values for latitude, solar radiation, VPD, and precipitation were below 2, indicating minimal collinearity (VIF<5; acceptable), demonstrating that each variable provides unique information. The right part of Fig. 7 shows the positive and negative impacts along with the quantitative contribution (better visible in the stacked column chart in the left part of the figure) of each independent variable to explain the variance in delta LST. The use of GAM in the integrated model analysis has enabled a clear classification of the independent variables' contributions to the delta LST into negative and positive effects.

Statistically, the model demonstrated strong predictive performance, evidenced by an R-squared value of 0.8326, indicating that the model explained approximately 83.26% of the variance in Delta-LST. The MAE and RMSE were calculated as 0.1583 and 0.1921, respectively, suggesting the model's predictions were close to the observed values. The significant p-values (<0.0001) for all features were observed, suggesting that each predictor had a statistically significant impact on delta LST.

The relative importance plot, derived from the RF model, reveals that VPD is the most significant contributor to delta LST (the temperature difference between built-up areas and tree-covered areas), accounting for 39% of the total contribution. The direction of influence indicates that VPD, as the dominant variable, has a negative impact, suggesting that drier conditions are associated with a decrease in delta LST. Followed by VPD, solar radiation positively influences delta LST, with a relative importance of 24%, indicating that increased solar radiation amplifies the temperature difference. Meanwhile, latitude also shows a significant impact, and precipitation has shown less contribution, probably because of the study time period, which witnessed contrasting precipitation patterns.

4. Discussions

One of the prerequisites for detailed thermal analysis at urban scale is the high-resolution thermal data with spatial variability. Therefore, this study has utilized regression-based model (GTB) that integrates high-resolution land use indices to downscale LST from 30 m to 10 m resolution. This allowed better attribution between thermal patterns and fine-scale LULC features, such as fragmented green spaces. Direct field-based validation would provide the most reliable accuracy assessment for the predicted high-resolution land surface temperature (LST). However, this study showed a strong statistical agreement. The high R-squared value and strong correlation with the original computed LST support the credibility of the downscaled LST data (Maraun et al., 2015; Rao et al., 2024a). This method is particularly suitable for studies where in-situ measurements are unavailable, allowing for a reasonable approximation of surface temperatures at finer spatial resolutions. It is to be noted here that this pixel-wise framework made GTB especially suitable given its flexibility and interpretability, as well as its efficiency in handling environmental data structures with high dimensionality but moderate sample sizes. More complex models such as CNNs (Convolutional Neural Networks), while powerful for image classification, were less appropriate here due to their reliance on large-scale image inputs and higher computational requirements, which were not aligned with our structured, tabular data setup. Also, aggregating predictions within larger zones (buffers) helped reduce local uncertainties and smooth high-frequency noise. This enhanced both statistical reliability and ecological relevance. This super-resolved LST has contributed to capturing the detailed thermal profiles of the land use land cover within the urban settings. It also supported quantifying UGS cooling effects across various geographic and climatic parameters, particularly along a small latitudinal gradient. This enhanced our understanding of UGS's role in mitigating UHI in different urban settings.

4.1. LULC distribution and surface temperature across urban gradients

Similar to the previous studies (Rahman et al., 2022; Rao, Tassinari, & Torreggiani, 2023), our study showed that the high built-up percentage near the city center progressively decreases towards the periphery, whereas the increased tree cover with distance from the center reflects the transition from dense urban cores to less built-up suburban zones. The mean LST (referred to daytime LST for this study) for 2022 and 2023 reveals a clear downward trend from the center towards the periphery in all cities, aligning with the corresponding increase and decline in tree cover and built-up areas. These results highlight the critical role of urban vegetation, particularly trees, in mitigating the UHI effect. As urban centers with high built-up densities exhibit the highest LST values (Rao & Gupta et al., 2021), tree cover becomes increasingly vital. The data further emphasizes integrating and maintaining substantial tree coverage in urban planning to combat rising city temperatures. Grasslands, despite contributing to green space, play a less significant role in temperature reduction (during daytime) compared to trees, whose shading and evapotranspiration processes make them far more effective in mitigating thermal stress (Rahman, Moser, Gold, Rötzer, & Pauleit, 2018; Rahman et al., 2020; Schwaab et al., 2021). This LULC distribution and LST trends set the stage for further exploration of the thermal contributions of different urban vegetation types, as examined in the following section. The subsequent discussion on the CI of trees and grasslands delves deeper into the spatial and latitudinal variations in vegetation's role in regulating urban microclimates. When considered alongside the LST and LULC data, these findings will provide a comprehensive understanding of how urban vegetation affects thermal dynamics at multiple spatial scales.

4.2. Role of urban morphology and vegetation types on cooling across urban gradients

The observed spatial variability in the CI of urban trees and grassland across the latitudinal gradient and urban-periphery transitions reflect microclimatic processes influenced by biophysical, urban morphological, and atmospheric factors. Urban trees and grasslands exhibit distinct microclimatic behaviors that influence their contribution to temperature regulation. Trees consistently demonstrate a more substantial cooling effect, driven by higher evapotranspiration rates and canopy shading, underscoring their substantial role in acting as thermal sinks of heat Franceschi et al. (2023), Gherri (2023). This effect is slightly more pronounced in 2023 for some cities due to the comparatively higher annual precipitation recorded in 2023, which contributes to changes in soil-moisture reserve and affects the cooling capacity of trees. Factors like tree species and canopy density also influence this cooling (Rötzer, Rahman, Moser-Reischl, Pauleit, & Pretzsch, 2019). However, information on tree species composition for the study areas is either unavailable or beyond the scope of this study. In contrast, grasslands exhibit a much weaker cooling influence on daytime urban LST, with CI values remaining close to zero in both years. This is attributed to lower evapotranspiration, extremely short canopy height, and limited moisture retention due to shallow root systems. Consequently, grasslands are less effective than trees in mitigating urban heat stress (Schwaab et al., 2021), at least where the grasses are not shaded (Rahman et al., 2021). These findings highlight the critical importance of tree cover in reducing thermal stress in cities, especially in densely populated areas. The minimal cooling impact of grasslands suggests that they should be integrated with other green infrastructure strategies to enhance urban cooling effectively (Rahman et al., 2021).

Cities at higher latitudes generally experience cooler summer temperatures and more humid and moister climates, resulting in enhanced cooling capabilities of vegetation and demonstrating their effectiveness as thermal sinks. Conversely, cities closer to lower latitudes often face hotter, drier summers, leading to a diminished cooling capacity of vegetation, as discussed earlier. In extreme instances, grassland shows even positive CI, since they quickly dry out with higher atmospheric demand and lower topsoil moisture (Gill, Rahman, Handley, & Ennos, 2013). Therefore, these cities might struggle with grassland in the future, requiring intensive green planning with tree cover. Careful consideration must be given when interpreting the results, particularly in relation to urban topography—such as street orientation—and the surrounding environment, including built geometry, urban design, and the proportion of green spaces, all of which significantly influence the mitigation of urban heat stress (Rahman et al., 2020). Sky View Factor, closely related to the urban canyon geometry, directly impacts solar exposure, shading duration, and wind flow, affecting evapotranspiration rates and shading efficiency. For instance, narrower street canyons can reduce evapotranspiration rates, which, in lower latitudes, may benefit urban heat mitigation, where transpiration is already limited due to high temperatures and vapor pressure deficit. Conversely, in higher-latitude cities (e.g., Hamburg, Hannover), buildings tend to be less compact, and green spaces are often more continuous and better ventilated, enhancing transpiration. In contrast, southern cities (e.g., Naples) typically exhibit denser urban fabrics, reduced wind penetration, and elevated VPD, which collectively constrain transpiration

processes. As a result, the cooling benefit of shade from trees becomes more critical than latent heat flux in these environments. Despite their strong mitigation potential, trees must be strategically placed to avoid obstructing major airflow pathways (Zölch, Rahman, Pfleiderer, Wagner, & Pauleit, 2019). Moreover, incorporating a diversified vegetation structure—both horizontally and vertically—can enhance the resilience and effectiveness of urban heat mitigation strategies (Wang et al., 2023).

4.3. Climatic interpretations of UGS surface thermal intensities and aridity trend within a narrow latitudinal range

As the study is focused on a small latitudinal gradient, which majorly falls under the temperate climate zones with generally similar vegetation types, the UGS thermal intensity and aridity trends can be attributed to subtle shifts in microclimatic conditions rather than major biome transitions. The vegetation within this gradient is of similar functional types, demonstrating effective cooling through evapotranspiration. However, in general, the cooling effect reduces while moving towards lower latitudes mainly due to the higher aridity. Higher aridity is witnessed in the southern part during summer, which reduces the cooling capacity of the UGS, especially grasslands. The rate of evapotranspiration is impacted due to low soil moisture, as in arid climates, trees perform reduced evapotranspiration during the high heat to reduce their hydraulic stress, resulting in decreased Delta-LST. As the latitude increases and DAI indicates lower aridity (closer to 53°N), more moisture supports greater evapotranspiration, resulting in increased cooling effect by trees. At the same time, vegetation, despite being of a similar functional type, remains more effective in the cooler and less arid northern part of the gradient, which becomes the opposite in the southern part and arid regions, thereby contributing to increased UHI effect (Lee, Mayer, & Chen, 2016). This variability suggests that local factors (e.g., climate, sky view factor, urban density, existing vegetation) significantly influence how different functional types of vegetation impact urban temperatures (Rahman et al., 2024).

Transpirational effectiveness is generally higher in higher-latitude cities with lower energy loads, as noted by Rahman et al. (2024); however; this is only true under conditions of low aridity. For instance, Würzburg, despite its higher latitude, experiences much drier conditions than Italian cities. Furthermore under high atmospheric demand, the cooling benefits of trees are primarily attributed to shading, and is readily admixed from the surrounding atmosphere and become less discernible while capturing LST. It is to be noted that the LST captures the surface-level thermal scenario, while transpirational cooling is more efficiently measured through leaf-level observations. Usually, transpirational cooling declines closer to the equator; the results indicate that atmospheric demand significantly influences cooling efficiency. This efficiency is determined not only by latitudinal position but also by geographical context.

4.4. Climatic contributors to urban thermal intensity and dynamics

The statistical modeling quantified the contribution of analyzed independent variables to the delta LST (difference in temperature between built-up and tree cover). It emphasized the complex interplay of climatic and geographical factors in shaping urban heat dynamics. Among these factors, VPD, a measure of air dryness and soil moisture, emerged as the most significant, influencing vegetation transpiration rates and affecting local thermal dynamics up to a certain threshold (Shashua-Bar et al., 2023). This phenomenon is common in cities with significant vegetation cover where trees can moderate temperature through transpiration. However, the cooling function of trees varies considerably based on the type of built-up design in heterogeneous urban landscapes (Pattnaik et al., 2024). Though it has been argued in the recent research that VPD is an important driver for transpirational cooling (Preisler et al., 2023), however, in this study we found that at large scale VPD is influencing negatively at stand level. The negative contribution of VPD to delta LST underscores the importance of maintaining UGS, typically in the era of rising temperatures associated with climate change. Notably, high VPD conditions reflect a drier atmosphere, limiting trees' cooling potential and making delta LST more dependent on other factors like solar radiation and local climatic conditions. Solar radiation was identified as the second most influential factor affecting delta LST. Higher latitudes, characterized by pronounced seasonal variations in solar radiation, influence thermal behavior of urban landscapes. For instance, cities in cooler climates at higher latitudes may have comparatively shorter growing seasons and less intense solar exposure. In contrast, built-up areas at lower latitudes retain more heat due to high intensity solar radiation (Oke, 1982). Latitude's impact reflects the cooling effects of milder climates and reduced radiative forcing at higher latitudes. Increased rainfall elevates moisture levels, enhances evapotranspiration, and contributes in heat load mitigation. Therefore, this study highlights that cooling benefits from similar green space types vary significantly across cities. This variation is primarily influenced by latitude-driven climatic factors, particularly vapor pressure deficit, solar radiation, and precipitation. These findings underscore the need for climate-sensitive and location-specific green infrastructure planning.

The LST in this study was derived from cloudless days, while VPD and transpiration operate as instantaneous processes. Higher transpiration rates are more closely linked to soil moisture reserves accumulated over the preceding days. Additionally, this analysis has been carried out on the typical summer days in 2 years with contrasting rainfall patterns (one almost dry and other wet), therefore are not truly represented, highlighting the scope for further research using time-series data to assess more scenarios with similar and/or varying precipitation patterns. This underscores urban planners' need to focus on moisture retention strategies and shade optimization in arid and high-VPD regions when designing green infrastructure.

4.5. Limitations of the study and future scope

The results highlight the effectiveness of the integrated model in capturing the complex interaction between the environmental variables and delta LST. Although solar radiation, VPD, and precipitation were directly measured, capturing specific climatic characteristics, other climatic and geographic factors (e.g., seasonal variations, land–sea contrasts, and altitude effects) are indirectly represented by latitude. Overall, the distinguished contribution of all the variables together serves as a broader geographic and climatic indicator, encompassing additional influences on temperature variations (Rahman et al., 2024). The findings underscore the utility of this modeling approach as a robust method for environmental modeling, particularly in settings where non-linear relationships are present and variable interactions are complex. However, it is essential to acknowledge the limitations of this study. The use of single-day LST data from peak summer periods does not capture seasonal or interannual variability in urban microclimates. Moreover, the training data quality and urban heterogeneity also play an important role in accurately predicting the high-resolution temperature data. Further, the statistical models used face notable limitations when applied to datasets with few data points. For example, GAMs may suffer from issues like overfitting and additivity assumption, while RF can struggle with generalization due to its "black box" nature (Simon, Glaum, & Valdovinos, 2023). Therefore, for this study, smoothing parameters were determined by running multiple model iterations to ensure robustness, and feature selections were made after considering the collinearity issue amongst the variables to mitigate bias. In addition, the analysis relied on cloud-free satellite data from similar days, which restricted our ability to compare a larger number of cities.

To overcome this, future research should focus on generating high spatial and temporal resolution thermal datasets, providing more detailed ground thermal information with good temporal coverage for

seasonal and annual analysis. A benchmark comparison with traditional resampling and downscaling methods (e.g.IDW, Kriging, which rely on spatial autocorrelation assumptions) would help validate and contextualize the results. Although this was beyond the scope of the present study, it can be addressed through broader model evaluations in future work. Also hybrid modeling approaches should be explored that combine interpretable models (e.g., GAM, RF) with deep learning methods, especially with larger, high-frequency datasets. Such advancements would facilitate analyses of cities across larger latitudinal gradients, encompassing a broader array of vegetation types and species compositions. In addition, incorporating urban morphological factors such as building height and street orientation, along with detailed vegetation classification, would be valuable for analyzing urban cooling impacts in upcoming research. The influence of groundwater and urban irrigation on vegetation cooling was not directly accounted for due to data limitations, and broader climatic indicators (like VPD, aridity index) were used as proxies for moisture availability. Examining the incorporation of additional variables or more complex modeling techniques to further enhance the understanding of the factors driving temperature changes is also a potential future scope.

5. Conclusions

This paper has proposed a less explored side of the urban environmental research, which is focused on quantifying the urban vegetation-led cooling in different cities with diverse climatic conditions, assuming similar vegetation composition across the latitudinal gradient. Our findings reveal that trees deliver a more pronounced cooling effect, particularly in densely populated urban areas, where their capacity for shading and evapotranspiration can significantly mitigate the UHI effect. This cooling efficiency is not uniform; it is significantly influenced by both latitudinal location and geographical positioning along with local climatic and landscape variables, such as temperature, precipitation, and urban morphology, which can vary widely even within small latitudinal ranges. Urban areas at higher latitudes (Northern part) experience high precipitation, increasing the moisture and increasing evapotranspirational cooling. Additionally, higher latitudes experience comparatively less solar intensity, therefore less heated urban areas, while lower latitudes (southern part) receive comparatively less rainfall and higher exposure to intense solar heat, contributing to drier climates, where trees contribute to reducing temperature more through their canopy density and crown shadowing than through evapotranspiration.

These research findings will help policymakers and urban planners prioritize strategic planting and selection of species, particularly in areas close to city centers, to effectively mitigate UHI effects, especially considering the future changed climatic scenarios. The study also indicates the need for continued monitoring and adaptive management of urban green spaces to maintain their cooling benefits over time. The approach of quantifying the cooling benefits of trees in different landscape settings can help plan cooler, healthier urban environments and contribute to the overall resilience of cities to climate change. In urban environments, there is a growing need for climate- and landscape-specific strategies to mitigate heat. For example, introducing drought-tolerant tree species with dense canopies in arid climates could provide better shading, particularly in lower-latitude cities, where urban heat is more pronounced. These global analyses, including more cities covering longer latitudinal gradients in future studies, would allow us to develop more robust prerequisites for the efficient planning of urban vegetation concerning the city's landscape characteristics and climatic conditions. The findings emphasize that urban green spaces do not offer uniform cooling benefits across different cities, even when similar in type. This variability, shaped by latitude-related climatic factors, suggests that green infrastructure strategies must be tailored to local environmental conditions. A one-size-fits-all approach can lead to suboptimal results in urban heat mitigation. Therefore, urban planning should prioritize location-specific assessments of green space performance. Incorporating high-resolution thermal analysis into planning processes can enhance the effectiveness of interventions. Hence, this detailed analysis supports efficient planning for urban cooling in various urban settings, thus contributing to healthier, more resilient, and livable future cities.

CRediT authorship contribution statement

Priyanka Rao: Writing – review & editing, Writing – original draft, Visualization, Validation, Methodology, Investigation, Formal analysis, Data curation, Conceptualization. **Daniele Torreggiani:** Writing – review & editing, Software, Resources, Project administration, Funding acquisition. **Patrizia Tassinari:** Writing – review & editing, Software, Resources, Funding acquisition. **Thomas Rötzer:** Writing – review & editing, Visualization, Investigation. **Stephan Pauleit:** Writing – review & editing, Software, Resources, Project administration, Investigation, Funding acquisition. **Mohammad A. Rahman:** Writing – review & editing, Visualization, Supervision, Project administration, Methodology, Investigation, Formal analysis, Conceptualization.

Declaration of competing interest

Neither financial nor any other substantive conflict of interest applies. No potential conflict of interest can be construed to have influenced the results or interpretation of the manuscript.

Appendix

Algorithm 1 Downscaling LST from 30m to 10m using GTB

Input: Landsat-8 image collection $\mathcal{L}$, Sentinel-2 image collection S, Region of Interest ROI, Date range $[t_1, t_2]$
Output: Downscaled LST at 10m resolution
Step 1: Preprocessing
(a) Apply cloud masking to $\mathcal{L}$ and S to remove cloudy pixels.
(b) Filter both collections by ROI and $[t_1, t_2]$.
Step 2: Compute Indices for Landsat-8 and Sentinel-2: NDVI, NDBI and NDWI
Step 4: Extract Landsat-8 LST: Compute Land Surface Temperature (LST) for Landsat-8 data and clip the LST image to ROI.
Step 5: Prepare Training Data
(a) Stack the computed indices and LST to create the Landsat-8 training dataset $\mathcal{D}_{train}$.
(b) Sample $\mathcal{D}_{train}$ within ROI at 10m scale to generate features and target values.
Step 6: Train Gradient Tree Boosting Model
for each pixel p in $\mathcal{D}_{train}$ **do**
Train the Gradient Tree Boosting (GTB) model using the indices as features and LST as the target.
end for
Step 7: Predict LST Using Sentinel-2 Data
for each pixel p in Sentinel-2 derived indices **do**
Apply the trained GTB model to predict LST at 10m resolution.
end for

Data availability

Data will be made available on request.

References

Abd-Elmabod, S. K., Gui, D., Liu, Q., Liu, Y., Al-Qthanin, R. N., Jiménez-González, M. A., et al. (2024). Seasonal environmental cooling benefits of urban green and blue spaces in arid regions. *Sustainable Cities and Society*, *115*, Article 105805.

Ayanlade, A., Aigbiremolen, M. I., & Oladosu, O. R. (2021). Variations in urban land surface temperature intensity over four cities in different ecological zones. *Scientific Reports*, *11*(1), 20537.

Balany, F., Ng, A. W., Muttil, N., Muthukumaran, S., & Wong, M. S. (2020). Green infrastructure as an urban heat island mitigation strategy—a review. *Water*, *12*(12), 3577.

Bartesaghi-Koc, C., Osmond, P., & Peters, A. (2020). Quantifying the seasonal cooling capacity of 'green infrastructure types'(GITs): An approach to assess and mitigate surface urban heat island in sydney, Australia. *Landscape and Urban Planning*, *203*, Article 103893.

Bowler, D. E., Buyung-Ali, L. M., Knight, T. M., & Pullin, A. S. (2010). A systematic review of evidence for the added benefits to health of exposure to natural environments. *BMC Public Health*, *10*, 1–10.

Bush, S. E., Pataki, D. E., Hultine, K. R., West, A. G., Sperry, J. S., & Ehleringer, J. R. (2008). Wood anatomy constrains stomatal responses to atmospheric vapor pressure deficit in irrigated, urban trees. *Oecologia*, *156*, 13–20.

Cao, X., Onishi, A., Chen, J., & Imura, H. (2010). Quantifying the cool island intensity of urban parks using ASTER and IKONOS data. *Landscape and Urban Planning*, *96*(4), 224–231.

Chen, J., Kinoshita, T., Li, H., Luo, S., Su, D., Yang, X., et al. (2023). Toward green equity: An extensive study on urban form and green space equity for shrinking cities. *Sustainable Cities and Society*, *90*, Article 104395.

Cheng, X., Peng, J., Dong, J., Liu, Y., & Wang, Y. (2022). Non-linear effects of meteorological variables on cooling efficiency of african urban trees. *Environment International*, *169*, Article 107489.

Cheung, P. K., Livesley, S. J., & Nice, K. A. (2021). Estimating the cooling potential of irrigating green spaces in 100 global cities with arid, temperate or continental climates. *Sustainable Cities and Society*, *71*, Article 102974.

Emilia-Romagna, R. (2024). Dexter. URL https://simc.arpae.it/dext3r/. (Accessed 12 July 2024).

Estoque, R. C., Murayama, Y., & Myint, S. W. (2017). Effects of landscape composition and pattern on land surface temperature: An urban heat island study in the megacities of Southeast Asia. *Science of the Total Environment*, *577*, 349–359.

Franceschi, E., Moser-Reischl, A., Honold, M., Rahman, M. A., Pretzsch, H., Pauleit, S., et al. (2023). Urban environment, drought events and climate change strongly affect the growth of common urban tree species in a temperate city. *Urban Forestry & Urban Greening*, *88*, Article 128083.

Gartland, L. M. (2012). *Heat islands: understanding and mitigating heat in urban areas*. Routledge.

Geoportal, L. R. (2024). RegioneLombardia. URL https://dati.lombardia.it/. (Accessed 12 July 2024).

Gherri, B. (2023). The role of urban vegetation in counteracting overheating in different urban textures. *Land*, *12*(12), 2100.

Gill, S., Rahman, M., Handley, J., & Ennos, A. (2013). Modelling water stress to urban amenity grass in manchester UK under climate change and its potential impacts in reducing urban cooling. *Urban Forestry & Urban Greening*, *12*(3), 350–358.

Guo, H.-D., Zhang, L., & Zhu, L.-W. (2015). Earth observation big data for climate change research. *Advances in Climate Change Research*, *6*(2), 108–117.

Hartmann, C., Moser-Reischl, A., Rahman, M. A., Franceschi, E., von Strachwitz, M., Pauleit, S., et al. (2023). The footprint of heat waves and dry spells in the urban climate of Würzburg, Germany, deduced from a continuous measurement campaign during the anomalously warm years 2018–2020. *Meteorologische Zeitschrift*.

Imhoff, M. L., Zhang, P., Wolfe, R. E., & Bounoua, L. (2010). Remote sensing of the urban heat island effect across biomes in the continental USA. *Remote Sensing of Environment*, *114*(3), 504–513.

Kim, J., Khouakhi, A., Corstanje, R., & Johnston, A. S. (2024). Greater local cooling effects of trees across globally distributed urban green spaces. *Science of the Total Environment*, *911*, Article 168494.

Kim, J., Yeom, S., & Hong, T. (2025). Analyzing the cooling effect, thermal comfort, and energy consumption of integrated arrangement of high-rise buildings and green spaces on urban heat island. *Sustainable Cities and Society*, *119*, Article 106105.

Koc, C. B., Osmond, P., & Peters, A. (2018). Evaluating the cooling effects of green infrastructure: A systematic review of methods, indicators and data sources. *Solar Energy*, *166*, 486–508.

Krayenhoff, E. S., Moustaoui, M., Broadbent, A. M., Gupta, V., & Georgescu, M. (2018). Diurnal interaction between urban expansion, climate change and adaptation in US cities. *Nature Climate Change*, *8*(12), 1097–1103.

Krishna, R. (1972). Remote sensing of urban heat islands from an environmental satellite.

Lee, H., Mayer, H., & Chen, L. (2016). Contribution of trees and grasslands to the mitigation of human heat stress in a residential district of Freiburg, Southwest Germany. *Landscape and Urban Planning*, *148*, 37–50.

Leong, D., Teo, K., Rangarajan, S., Lopez-Jaramillo, P., Avezum, A., Jr., Orlandini, A., et al. (2018). World population prospects 2019. Department of economic and social affairs population dynamics. New york (NY): United nations; 2019 (, accessed 20 september 2020). The decade of healthy ageing. Geneva: World Health Organization. *World*, *73*(7), 362k2469,.

Li, Z.-L., & Duan, S.-B. (2018). Land surface temperature. *Comprehensive Remote Sensing*, *5*, 264–283.

Li, Y., Svenning, J.-C., Zhou, W., Zhu, K., Abrams, J. F., Lenton, T. M., et al. (2024). Green spaces provide substantial but unequal urban cooling globally. *Nature Communications*, *15*(1), 7108.

Liu, Y., Chen, H., Wu, J., Wang, Y., Ni, Z., & Chen, S. (2024). Impact of urban spatial dynamics and blue-green infrastructure on urban heat islands: A case study of Guangzhou using local climate zones and predictive modeling. *Sustainable Cities and Society*, *115*, Article 105819.

Manoli, G., Fatichi, S., Schläpfer, M., Yu, K., Crowther, T. W., Meili, N., et al. (2019). Magnitude of urban heat islands largely explained by climate and population. *Nature*, *573*(7772), 55–60.

Maraun, D., Widmann, M., Gutiérrez, J. M., Kotlarski, S., Chandler, R. E., Hertig, E., et al. (2015). VALUE: A framework to validate downscaling approaches for climate change studies. *Earth's Future*, *3*(1), 1–14.

Martin-StPaul, N., Delzon, S., & Cochard, H. (2017). Plant resistance to drought depends on timely stomatal closure. *Ecology Letters*, *20*(11), 1437–1447.

Mavrakis, A., & Papavasileiou, H. (2013). NDVI and E. de martonne indices in an environmentally stressed area (Thriasio Plain–Greece). *Procedia Technology*, *8*, 477–481.

Mora, C., Dousset, B., Caldwell, I. R., Powell, F. E., Geronimo, R. C., Bielecki, C. R., et al. (2017). Global risk of deadly heat. *Nature Climate Change*, *7*(7), 501–506.

Oke, T. R. (1982). The energetic basis of the urban heat island. *Quarterly Journal of the Royal Meteorological Society*, *108*(455), 1–24.

Oren, R., Sperry, J., Katul, G., Pataki, D., Ewers, B., Phillips, N., et al. (1999). Survey and synthesis of intra-and interspecific variation in stomatal sensitivity to vapour pressure deficit. *Plant, Cell & Environment*, *22*(12), 1515–1526.

Pardo, S. K., & Paredes-Fortuny, L. (2024). Uneven evolution of regional European summer heatwaves under climate change. *Weather and Climate Extremes*, *43*, Article 100648.

Pattnaik, N., Honold, M., Franceschi, E., Moser-Reischl, A., Rötzer, T., Pretzsch, H., et al. (2024). Growth and cooling potential of urban trees across different levels of imperviousness. *Journal of Environmental Management*, *361*, Article 121242.

Paudel, I., Naor, A., Gal, Y., & Cohen, S. (2015). Simulating nectarine tree transpiration and dynamic water storage from responses of leaf conductance to light and sap flow to stem water potential and vapor pressure deficit. *Tree Physiology*, *35*(4), 425–438.

Portal, C. R. (2024). Campania weather data dashboard. URL https://centrofunzionale.regione.campania.it#pages/dashboard. (Accessed 12 July 2024).

Preisler, Y., Grünzweig, J. M., Ahiman, O., Amer, M., Oz, I., Feng, X., et al. (2023). Vapour pressure deficit was not a primary limiting factor for gas exchange in an irrigated, mature dryland Aleppo pine forest. *Plant, Cell & Environment*, *46*(12), 3775–3790.

Pyrgou, A., Hadjinicolaou, P., & Santamouris, M. (2020). Urban-rural moisture contrast: Regulator of the urban heat island and heatwaves' synergy over a mediterranean city. *Environmental Research*, *182*, Article 109102.

Rahman, M. A., Arndt, S., Bravo, F., Cheung, P. K., van Doorn, N., Franceschi, E., et al. (2024). More than a canopy cover metric: Influence of canopy quality, water-use strategies and site climate on urban forest cooling potential. *Landscape and Urban Planning*, *248*, Article 105089.

Rahman, M. A., Dervishi, V., Moser-Reischl, A., Ludwig, F., Pretzsch, H., Rötzer, T., et al. (2021). Comparative analysis of shade and underlying surfaces on cooling effect. *Urban Forestry & Urban Greening*, *63*, Article 127223.

Rahman, M. A., Franceschi, E., Pattnaik, N., Moser-Reischl, A., Hartmann, C., Paeth, H., et al. (2022). Spatial and temporal changes of outdoor thermal stress: influence of urban land cover types. *Scientific Reports*, *12*(1), 671.

Rahman, M. A., Moser, A., Gold, A., Rötzer, T., & Pauleit, S. (2018). Vertical air temperature gradients under the shade of two contrasting urban tree species during different types of summer days. *Science of the Total Environment*, *633*, 100–111.

Rahman, M. A., Moser, A., Rötzer, T., & Pauleit, S. (2019). Comparing the transpirational and shading effects of two contrasting urban tree species. *Urban Ecosystems*, *22*, 683–697.

Rahman, M. A., Stratopoulos, L. M., Moser-Reischl, A., Zölch, T., Häberle, K.-H., Rötzer, T., et al. (2020). Traits of trees for cooling urban heat islands: A meta-analysis. *Building and Environment*, *170*, Article 106606.

Rao, P., Gupta, K., Roy, A., & Balan, R. (2021). Spatio-temporal analysis of land surface temperature for identification of heat wave risk and vulnerability hotspots in Indo-Gangetic Plains of India. *Theoretical and Applied Climatology*, *146*(1), 567–582.

Rao, P., Singh, A., & Pandey, K. (2021). Time-series analysis of open data for studying urban heat island phenomenon: a geospatial approach. *Spatial Information Research*, *29*, 907–918.

Rao, P., Tassinari, P., & Torreggiani, D. (2023). Exploring the land-use urban heat island nexus under climate change conditions using machine learning approach: A spatio-temporal analysis of remotely sensed data. *Heliyon*, *9*(8).

Rao, P., Tassinari, P., & Torreggiani, D. (2024a). Evaluating land use indices contribution for super-resolving surface temperature: An ablation study. In *IGARSS 2024-2024 IEEE international geoscience and remote sensing symposium* (pp. 4040–4043). IEEE.

Rao, P., Tassinari, P., & Torreggiani, D. (2024b). A framework analyzing climate change, air quality and greenery to unveil environmental stress risk hotspots. *Remote Sensing*, *16*(13), 2420.

Rao, P., Tassinari, P., & Torreggiani, D. (2024c). Unveiling climate dynamics: An in-depth analysis of temperature anomalies in Italian climatic regions. In *IGARSS 2024-2024 IEEE international geoscience and remote sensing symposium* (pp. 3889–3892). IEEE.

Rötzer, T., Rahman, M., Moser-Reischl, A., Pauleit, S., & Pretzsch, H. (2019). Process based simulation of tree growth and ecosystem services of urban trees under present and future climate conditions. *Science of the Total Environment*, *676*, 651–664.

Saaroni, H., Amorim, J. H., Hiemstra, J., & Pearlmutter, D. (2018). Urban green infrastructure as a tool for urban heat mitigation: Survey of research methodologies and findings across different climatic regions. *Urban Climate*, *24*, 94–110.

Schwaab, J., Meier, R., Mussetti, G., Seneviratne, S., Bürgi, C., & Davin, E. L. (2021). The role of urban trees in reducing land surface temperatures in European cities. *Nature Communications*, *12*(1), 6763.

Seager, R., Osborn, T. J., Kushnir, Y., Simpson, I. R., Nakamura, J., & Liu, H. (2019). Climate variability and change of mediterranean-type climates. *Journal of Climate*, *32*(10), 2887–2915.

Service, G. N. M. (2024a). Deutscher wetterdienst. URL https://opendata.dwd.de/climate_environment/CDC/observations_germany/. (Accessed 12 July 2024).

Service, H. N. M. (2024b). HungaroMet. URL https://odp.met.hu/climate/observations_hungary/. (Accessed 12 July 2024).

Shashua-Bar, L., Rahman, M. A., Moser-Reischl, A., Peeters, A., Franceschi, E., Pretzsch, H., et al. (2023). Do urban tree hydraulics limit their transpirational cooling? A comparison between temperate and hot arid climates. *Urban Climate*, *49*, Article 101554.

Sheng, S., & Wang, Y. (2024). Configuration characteristics of green-blue spaces for efficient cooling in urban environments. *Sustainable Cities and Society*, *100*, Article 105040.

Simon, S. M., Glaum, P., & Valdovinos, F. S. (2023). Interpreting random forest analysis of ecological models to move from prediction to explanation. *Scientific Reports*, *13*(1), 3881.

Tejedor, E., Benito, G., Serrano-Notivoli, R., González-Rouco, F., Esper, J., & Büntgen, U. (2024). Recent heatwaves as a prelude to climate extremes in the western mediterranean region. *Npj Climate and Atmospheric Science*, *7*(1), 218.

Thome, K. (2001). Absolute radiometric calibration of Landsat 7 ETM+ using the reflectance-based method. *Remote Sensing of Environment*, *78*(1–2), 27–38.

Tran, H., Uchihama, D., Ochi, S., & Yasuoka, Y. (2006). Assessment with satellite data of the urban heat island effects in Asian mega cities. *International Journal of Applied Earth Observation and Geoinformation*, *8*(1), 34–48.

Varquez, A., & Kanda, M. (2018). Global urban climatology: A meta-analysis of air temperature trends (1960–2009). npj climate and atmospheric science, 1 (1), 32.

Wang, X., Rahman, M. A., Mokroš, M., Rötzer, T., Pattnaik, N., Pang, Y., et al. (2023). The influence of vertical canopy structure on the cooling and humidifying urban microclimate during hot summer days. *Landscape and Urban Planning*, *238*, Article 104841.

Weng, Q. (2009). Thermal infrared remote sensing for urban climate and environmental studies: Methods, applications, and trends. *ISPRS Journal of Photogrammetry and Remote Sensing*, *64*(4), 335–344.

Wulder, M. A., White, J. C., Loveland, T. R., Woodcock, C. E., Belward, A. S., Cohen, W. B., et al. (2016). The global landsat archive: Status, consolidation, and direction. *Remote Sensing of Environment*, *185*, 271–283.

Xu, J., Jin, Y., Ling, Y., Sun, Y., & Wang, Y. (2025). Exploring the seasonal impacts of morphological spatial pattern of green spaces on the urban heat island. *Sustainable Cities and Society*, Article 106352.

Yao, Y., Chang, C., Ndayisaba, F., & Wang, S. (2020). A new approach for surface urban heat island monitoring based on machine learning algorithm and spatiotemporal fusion model. *IEEE Access*, *8*, 164268–164281.

Yue, W., Liu, X., Zhou, Y., & Liu, Y. (2019). Impacts of urban configuration on urban heat island: An empirical study in China mega-cities. *Science of the Total Environment*, *671*, 1036–1046.

Zhang, Y., Ge, J., Wang, S., & Dong, C. (2025). Optimizing urban green space configurations for enhanced heat island mitigation: A geographically weighted machine learning approach. *Sustainable Cities and Society*, *119*, Article 106087.

Zhao, L., Li, T., Przybysz, A., Liu, H., Zhang, B., An, W., et al. (2023). Effects of urban lakes and neighbouring green spaces on air temperature and humidity and seasonal variabilities. *Sustainable Cities and Society*, *91*, Article 104438.

Zhu, W., Sun, J., Yang, C., Liu, M., Xu, X., & Ji, C. (2021). How to measure the urban park cooling island? A perspective of absolute and relative indicators using remote sensing and buffer analysis. *Remote Sensing*, *13*(16), 3154.

Zölch, T., Rahman, M. A., Pfleiderer, E., Wagner, G., & Pauleit, S. (2019). Designing public squares with green infrastructure to optimize human thermal comfort. *Building and Environment*, *149*, 640–654.